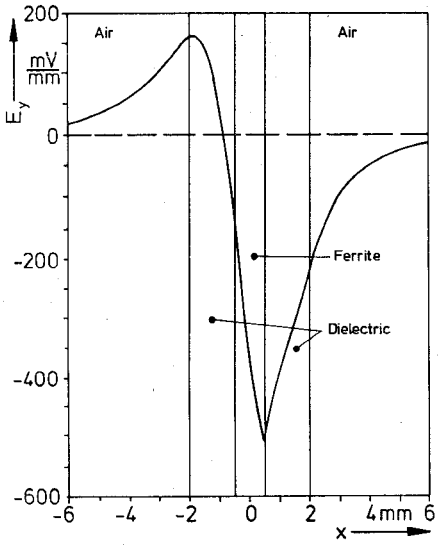

Fig. 5. The x dependence of the y component of the electric field strength of the superposition of the two modes from Figs. 3 and 4 at $z = 0$.

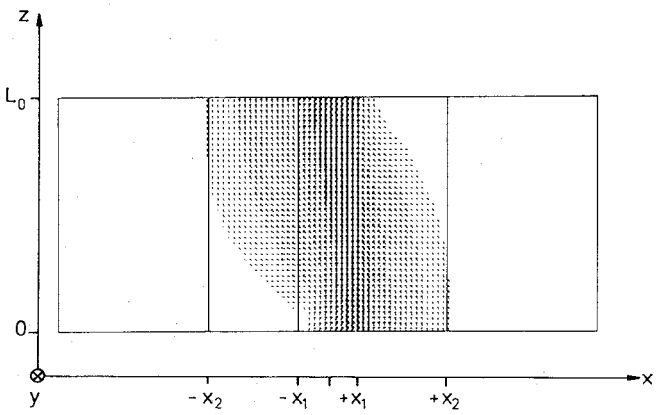

Fig. 6. Longitudinal power flow (Poynting vector) of the superposition of the two fundamental modes.

III. Principal Results

From (15) the power division factor k may become larger than one, in which case the power transported on guide A is negative. This means that the power on this transmission line is transported in the $-z$ direction. Nevertheless, inspecting both guides together the power transport still goes in the $+z$ direction. If k is less than or equal to one, the magnitudes of the scattering parameters at $z = l$ can be determined:

$$|S_{21}| = \sqrt{P_A(z=l)/P_0} = \sqrt{\{1+k\cos(\pi l/L)\}/\{1+k\}} \quad (18)$$

$$|S_{31}| = \sqrt{P_B(z=l)/P_0} = \sqrt{\{k-k\cos(\pi l/L)\}/\{1+k\}}\,. \quad (19)$$

Fig. 2 shows a diagram of the scattering parameters versus the normalized coupler length for a power division factor $k = 0.8$. Because the magnitude of S_{21} never becomes equal to zero, it can be recognized that an incomplete periodical coupling is submitted.

The phases of the S parameters can be calculated from the electromagnetic fields ((4) and (5)). It has been assumed that they have zero phases for $z = 0$. Therefore the phases of these fields at $z = l$ and at significant coordinates (x, y) of each line are equal to the phases of the corresponding scattering parameters.

If the structure is electromagnetically symmetric, $P_A^{I,I}$ and $P_B^{I,I}$, as well as $P_A^{II,II}$ and $P_B^{II,II}$, are identical. This implies that k becomes one. Thus (18) and (19) of this generalized theory converge into (1) and (2) of the common coupler theory.

The x dependences for the E_y field components of the first two single modes on the guide are shown in Figs. 3 and 4. The superposition of these two modes described above is shown in Fig. 5. The resulting power flow in the z direction is shown in Fig. 6. At $z = 0$ no part of the power is transported between $-x_2 \leqslant x \leqslant -x_1$. For increasing values of z, part of the power flow changes to this line, but at $z = L_0$ a nonnegligible part of the power is still transported between $+x_1 \leqslant x \leqslant +x_2$. This demonstrates the incomplete coupling at electromagnetically asymmetrical coupled lines.

IV. Conclusions

The method presented here is an extension of the well-known even- and odd-mode analysis for symmetrical coupled lines. The power consideration allows an integral formulation of the problem and can also be used for asymmetrical problems. In these cases the coupling is incomplete in the sense that only a part of the total power is coupled between the two guides. The principles of such coupler applications have been demonstrated using the example of an image guide coupler with a premagnetized ferrite slab.

References

[1] L. Young, *Parallel Coupled Lines and Directional Couplers*. Dedham, MA: Artech House, 1972.

[2] F. Arndt, B. Koch, H.-J. Orlok, and N. Schröder, "Field theory design of rectangular waveguide broad-wall metal-insert slot couplers for millimeter-wave applications," *IEEE Trans. Microwave Theory Tech.*, vol. MTT-33, pp. 95–104, Feb. 1985.

[3] V. K. Tripathi and Y. K. Chin, "Analysis of the general nonsymmetrical directional coupler with arbitrary terminations," *Proc. Inst. Elec. Eng.*, vol. 129, pt. H, no. 6, pp. 360–362, Dec. 1982.

[4] P. K. Ikäläinen, G. L. Matthaei, and M. M. Monte, "Broadband dielectric waveguide 3 dB-couplers using asymmetrical coupled lines," *IEEE MTT-S Int. Microwave Symp. Dig.* (Baltimore) 1985, pp. 135–138.

[5] A. Nicol and L. E. Davis, "Nonreciprocal coupling in dielectric image lines," *Proc. Inst. Elec. Eng.*, vol. 132, pt. H, no. 4, pp. 269–270, July 1985.

[6] D. Köther, I. Wolff, and A. Beyer, "A field theoretical analysis of ferrite-loaded image line isolators for the *Ka*-band," in *Proc. 15th European Microwave Conf.* (Paris), Sept. 1985, pp. 831–836.

[7] D. Köther, and A. Beyer, "Analysis of higher order modes on unilateral finlines with arbitrarily located slots," *Int. J. Infrared and Millimeter Waves*, vol. 7, no. 7, pp. 1037–1045, July 1986.

Improved Theory for E-Plane Symmetrical Tee Junctions

TSUNEHIRO OBATA AND JIRO CHIBA, MEMBER, IEEE

***Abstract*—We examine Lewin's theory, which describes an E-plane symmetrical tee junction by a peculiar equivalent circuit with only three parameters. It is shown that although his theory is formally correct, its circuit parameters depend on the amplitudes of reflected waves. An improved theory corrects this fault.**

Manuscript received November 11, 1987; revised October 10, 1988.

The authors are with the Department of Electrical Engineering, Tohoku University, Sendai 980, Japan.

IEEE Log Number 8825373.

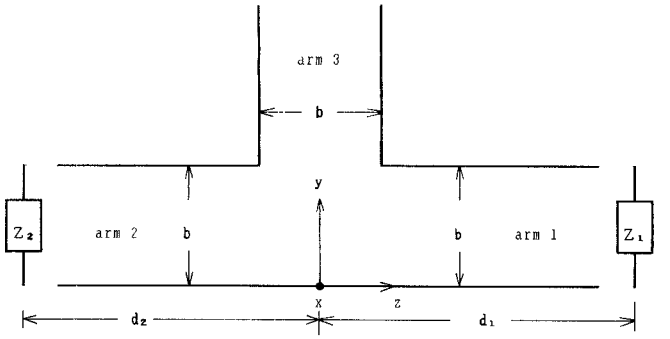

Fig. 1. E-plane T junction, longitudinal section. Lewin's theory imposes the terminal condition that there be loads at $z = d_1$ and $-d_2$ and that the ingoing wave fed from the upper arm have an E_z of unit amplitude at $y = b$. On the other hand, our theory does not use such specific boundary conditions.

I. Introduction

Various circuit parameters for tee junctions have been proposed. Let us consider some typical examples. Allanson, Cooper, and Cowling (ACC) [1] proposed a simple equivalent circuit for tee junctions by using the idea of characteristic points. If the reference planes are located at characteristic points, ACC's equivalent circuit is composed of only a transformer and a reactance. For an E-plane symmetrical tee and an H-plane symmetrical tee, they determined the four parameters of two characteristic points, the winding ratio of the transformer, and the reactance, employing a method suggested by Frank and Chu [2]. Sharp [3] devised an excellent method of analyzing the electric performance of tees having arbitrary cross sections. This method yields an admittance matrix. For symmetrical tees, he determined four independent elements of the admittance matrix. Marcuvitz [4] adopted a variational approach for E-plane symmetrical tees and H-plane symmetrical tees. The stationary values yield three admittances of a π-type equivalent circuit consisting of four admittances. The remaining one is determined by the equivalent static method. From the π-type elements, he also calculated ACC's parameters and so on. Lewin [5] also treated variational equations for an E-plane symmetrical tee, and gave a peculiar equivalent circuit described by only three parameters. However, he did not make any numerical calculation of the three parameters.

The tees above are symmetric. Generally, any symmetrical tee supporting only the fundamental mode can be described by four independent parameters. In fact, we have seen in the above that ACC, Sharp, and Marcuvitz described symmetrical tees by four parameters. On the other hand, Lewin represented the E-plane symmetrical tee of Fig. 1 by a peculiar equivalent circuit with only three parameters. This seems to be curious. The present paper reexamines Lewin's theory. We show that although his theory is formally correct, his circuit parameters depend on the amplitudes of waves reflected on the loads of Fig. 1. We give an improved theory. Our theory yields the circuit equations in a hybrid representation whose matrix has four independent elements. The circuit equations produce a simple equivalent circuit (Fig. 2) that is composed of two parts of a two-port circuit and a one-port circuit. According to the numerical calculation of the hybrid matrix, its determinant is nearly equal to zero, so the number of independent hybrid elements reduces to approximately three. The element l_{ee} of Fig. 2 then vanishes. In the case of $l_{ee} = 0$, Fig. 2 is equivalent to Lewin's equivalent circuit. Thus Lewin's equivalent circuit with only three parameters holds approximately.

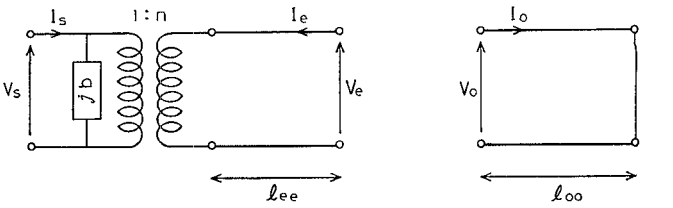

Fig. 2 An equivalent circuit based on the circuit equations (18a) and (18b), which is composed of two parts of a two-port circuit and a one-port circuit: $\tan \kappa l_{ee} = (H_{se}^2 - H_{ss}H_{ee})/H_{ss}$, $n^2 = (H_{se}/H_{ss})^2/(1 + \tan^2 \kappa l_{ee})$, $b = 1/H_{ss} - n^2 \tan \kappa l_{ee}$, $\tan \kappa l_{oo} = 1/H_{oo}$. Lewin's equivalent circuit does not have the element l_{ee}, and his circuit elements B_0, B_1, and K^2 correspond to our b, $\tan \kappa l_{oo}$, and $2n^2$, respectively. (Lewin originally described the tee by a three-port circuit. The equivalence of the two circuits is easily ascertained by examining their response to excitations which are even or odd with respect to the z coordinate.)

II. Lewin's Theory

Let us briefly review Lewin's theory for the tee of Fig. 1, and point out that his circuit parameters depend on the amplitudes of waves reflected on the loads. He decomposes the junction field $E(z) \equiv [E_z(y, z)]_{y=b}$ into the even part $f(z)$ and the odd part $g(z)$; $E(z) = f(z) + g(z)$. The $f(z)$ and $g(z)$ are determined by the integral equations obtained from a continuity condition at the junction plane:

$$(A - B - f)\cos \kappa z + 1 - R = j\kappa \int_0^{b/2} f(z')\{G_{\text{junc}}(z; z') + G_{\text{junc}}(z; -z')\}\, dz' \quad \text{(1a)}$$

$$(A + B + jg)\sin \kappa z = \kappa \int_0^{b/2} g(z')\{G_{\text{junc}}(z; z') - G_{\text{junc}}(z; -z')\}\, dz' \quad \text{(1b)}$$

with

$$G_{\text{junc}}(z; z') \equiv -\frac{\sin \kappa |z - z'|}{2\kappa b} + \sum_{n=1} \frac{\exp(-\Gamma_n |z - z'|)}{\Gamma_n b} + 2 \sum_{n=1} \frac{\cos[n\pi/b(z + b/2)] \cos[n\pi/b(z' + b/2)]}{\Gamma_n b} \quad (2)$$

$$\Gamma_n \equiv \left[(n\pi/b)^2 - \kappa^2\right]^{1/2}.$$

Here κ is the propagation constant of the fundamental mode. R is the reflection coefficient from the junction in the upper arm, and it is referred to $y = b$. It can be expressed in terms of the junction field:

$$(1 + R)/2 = 1/b \int_0^{b/2} f(z')\, dz' \equiv h. \quad (3)$$

The quantities f and g are constants defined by the junction field:

$$f \equiv 1/b \int_0^{b/2} f(z') \cos \kappa z'\, dz' \quad \text{(4a)}$$

$$g \equiv 1/b \int_0^{b/2} g(z') \sin \kappa z'\, dz'. \quad \text{(4b)}$$

A and B are the E_y amplitudes of the reflected and the propagating wave in the right arm and the left arm, respectively. Both amplitudes are referred to the $z = 0$ plane. They can also be

expressed in terms of the junction field:

$$B - A + f = [f(1-R_1)(1-R_2) + jg(R_2 - R_1)]/(1 - R_1R_2) \tag{5a}$$

$$-j(A+B) + g = [g(1+R_1)(1+R_2) + jf(R_2 - R_1)]/(1 - R_1R_2). \tag{5b}$$

R_1 and R_2 are the reflection coefficients from the loads, and they are referred to the $z = 0$ plane:

$$R_i = [(Z_i - 1)/(Z_i + 1)] \exp(-2jkd_i), \qquad i = 1,2.$$

From the above equations, Lewin derives the following equation for the normalized input admittance $Y = (1-R)/(1+R)$ at $y = b$ in the upper arm:

$$Y = jB_0 + 1/2K^2 \cdot [1/2(Y_1 + Y_2) + jB_1Y_1Y_2]/[1 + 1/2jB_1(Y_1 + Y_2)] \tag{6}$$

where the "circuit elements" B_0, B_1, and K^2 are given by

$$B_0 = (k/2h^2b^2) \int_0^{b/2} dz' \int_0^{b/2} dz f(z') f(z) b \cdot \{G_{\text{junc}}(z; z') + G_{\text{junc}}(z; -z')\} \tag{7a}$$

$$B_1 = (k/b^2g^2) \int_0^{b/2} dz' \int_0^{b/2} dz\, g(z') g(z) b \cdot \{G_{\text{junc}}(z; z') - G_{\text{junc}}(z; -z')\} \tag{7b}$$

$$K^2 = f^2/h^2. \tag{7c}$$

Equation (6) for the input admittance yields Lewin's equivalent circuit (see Fig. 2).

All the equations above are valid. However, as will be proved in the following, B_0 and K^2 depend on the amplitudes of reflected waves. Thus it is impossible to regard B_0 and K^2 as circuit elements, because the circuit elements of any linear waveguide should be independent of their excitation amplitudes. We now prove this fact.

The load admittances Y_1 and Y_2 or their reflection coefficients R_1 and R_2 are known. The amplitudes A and B are unknown constants, which will be determined after the integral equations are solved. Instead of this boundary condition, we can first give an amplitude of the reflected wave in the right arm, and the one in the left arm, for instance, A and B. In this case, A and B appearing in the integral equations (1a) and (1b) are previously given constants. Y_1, Y_2 or R_1, R_2 are then unknown constants, which will be determined after the integral equations are solved.

We now choose A and B as independent known constants. Taking account of (3) and (4a), we see from (1a) that $f(z)$ is linear with respect to $(A - B)$. Equations (1b) and (4b) yield that $g(z)$ is proportional to $(A + B)$. So we can write

$$f(z) = f_0(z) + (A - B) f_1(z) \tag{8a}$$

$$g(z) = (A + B) g_1(z) \tag{8b}$$

where $f_0(z)$, $f_1(z)$, and $g_1(z)$ are independent of A and B. Substituting (8b) into (7b) and (4b), we see that B_1 is independent of A and B. If $f_0(z) = 0$, the same is true of B_0 and K^2. However, this cannot happen. It is possible to put $A = B = 0$ as a boundary condition, that is, no reflected waves in the right and left arms. Supposing $f_0(z) = 0$, we then have $R = -1$ from (3). So (1a) gets reduced to the contradictory equation $2 = 0$. Thus we conclude that $f_0(z) \neq 0$. Accordingly in (7a) and (7c) for B_0 and K^2, the $(A - B)$ involved in the numerators and that in the denominators cannot cancel each other. In other words, B_0 and K^2 depend on $(A - B)$.

Lewin's treatment has such a contradiction. Nonetheless we would like to stress that his equivalent circuit holds approximately. This fact and a satisfying treatment will be given in the next section.

III. An Improved Theory

Our theory for the E-plane tee will not use any specific boundary condition such as the load admittances, so the theory holds in any boundary condition. We introduce voltage and current according to Schwinger [6]: current I_i as the lowest mode part of $-(\omega\mu/\kappa^2)H_x$ with angular frequency ω and magnetic permeability μ, and voltage V_i as the integral of the electric field across the ith arm multiplied by ± 1 (+ for $i = 2$, − for $i = 1,3$). We then have the characteristic impedance of $Z \equiv 1/Y \equiv \kappa b$. They refer to the same planes of $y = b$ and $z = 0$ as Lewin's planes. We also define six linear combinations as follows:

$$\begin{aligned} V_s &\equiv V_3/\sqrt{Z} & V_e &\equiv (V_2 + V_1)/\sqrt{2Z} & V_o &\equiv (V_2 - V_1)/\sqrt{2Z} \\ I_s &\equiv I_3/\sqrt{Y} & I_e &\equiv (I_2 + I_1)/\sqrt{2Y} & I_o &\equiv (I_2 - I_1)/\sqrt{2Y}. \end{aligned} \tag{9}$$

We can freely control three independent linear combinations. Our theory chooses I_s, I_e, and V_o for the three combinations, and we expand the junction field $E(z)$ in terms of them:

$$jE(z) = \kappa(\epsilon_s(z) I_s + \epsilon_e(z) I_e - j\epsilon_o(z) V_o). \tag{10}$$

It is easy to verify that $\epsilon_s(z)$ and $\epsilon_e(z)$ are even functions and that $\epsilon_o(z)$ is an odd function. The continuity of H_x at the junction then yields three integral equations for $\epsilon_M(z)$, $M = s, e, o$:

$$f_M(z) = \kappa \int_{-b/2}^{b/2} G_{\text{junc}}(z; z') \epsilon_M(z')\, dz' \tag{11}$$

with

$$f_M(z) \equiv \begin{cases} \sqrt{Y}, & M = s \\ -\sqrt{Y/2} \cos \kappa z, & M = e \\ -\sqrt{Y/2} \sin \kappa z, & M = o. \end{cases} \tag{12}$$

Equations (11) can be easily transformed into variational equations by a standard method:

$$B_M = \frac{\kappa^2 \int_{-b/2}^{b/2} dz \int_{-b/2}^{b/2} dz' G_{\text{junc}}(z; z') \epsilon_M(z) \epsilon_M(z')}{\left[\kappa \int_{-b/2}^{b/2} dz f_M(z) \epsilon_M(z)\right]^2} \tag{13}$$

with

$$1/B_M \equiv \kappa \int_{-b/2}^{b/2} f_M(z) \epsilon_M(z)\, dz. \tag{14}$$

Any asymptotic field components can be expressed in terms of the junction field $E(z)$ and I_M, V_M, $M = s, e, o$. Combining the expression with the decomposition (10), we obtain the circuit equations in a hybrid representation:

$$\begin{bmatrix} V_s \\ V_e \end{bmatrix} = -j \begin{bmatrix} H_{ss} & H_{se} \\ H_{es} & H_{ee} \end{bmatrix} \begin{bmatrix} I_s \\ I_e \end{bmatrix} \tag{15a}$$

$$I_o = -jH_{oo} V_o \tag{15b}$$

TABLE I
THEORETICAL CONSTANTS FOR THE E-PLANE SYMMETRICAL T JUNCTION

	hybrid elements				(HssHee-Hse²)/Hss
b/λg	Hss	2 Hee	√2 Hse	Hoo	(= -tan κ lee)
0.01	218.	218	-218.	0.00465	0
0.05	42.3	41.9	-42.1	0.0231	0.0
0.10	19.3	18.6	-18.9	0.0452	0.0
0.15	11.2	10 2	-10.7	0.0655	0 0
0.20	7.06	6.02	-6.51	0 0825	0.01
0.25	4.63	3 61	-4.08	0.0960	0 0i
0.30	3.08	2.17	-2.57	0.104	0.01
0.35	2.04	1 28	-1 59	0.105	0 02
0.40	1.30	0.729	-0.934	0.0985	0 029
0 425	0.994	0.535	-0.683	0 0915	0 033
0 45	0.713	0.378	-0.465	0.0795	0 037

with

$$H_{MN} \equiv \kappa \int_{-b/2}^{b/2} f_M(z)\,\epsilon_N(z)\,dz \qquad (M, N = s, e, o). \quad (16)$$

It is easily proved with the aid of (11) that the hybrid matrix is symmetric: $H_{MN} = H_{NM}$. The consideration of the parity of $f_M(z)$ and $\epsilon_N(z)$ immediately produces $H_{so} = H_{eo} = 0$. So the hybrid matrix has four independent elements. Note that the diagonal elements are equal to the inverse stationary values: $H_{MM} = 1/B_M$. On the basis of the circuit equations (15a) and (15b) we can represent the E-plane tee by a two-port circuit and a one-port circuit. Fig. 2 is an example.

The numerical analysis of (11) and (16) produces Table I. Here $\lambda_g \equiv 2\pi/\kappa$. The last column represents the determinant of the matrix in (15a) divided by H_{ss}, which is equal to $-\tan \kappa l_{ee}$ in Fig. 2. Each value of this table is accurate to within an error of ± 1 in its last place over most of $0 < b/\lambda_g < 0.5$. Using this table, we can calculate the parameters of Fig. 2, ACC's parameters, Sharp's admittance parameters, and so on. We have ascertained that our calculation of ACC's characteristic points coincides with ACC's data [1, table 2] to within 0.4 percent over most of $0 < b/\lambda_g < 0.5$. This agreement is seen to be excellent, and it can be concluded that our numerical analysis is verified by the independent result. The table suggests

$$H_{ee}/H_{ss} \to 1/2 \qquad H_{se}/H_{ss} \to -1/\sqrt{2} \qquad \text{for } b/\lambda_g \to 0. \quad (17)$$

Although the number of figures in the last column is not sufficient for small values of b/λ_g, eq. (17) leads to $(H_{ss}H_{ee} - H_{se}^2) \to 0$, so $\tan \kappa l_{ee} \to 0$. Noting this asymptotic behavior, we can conclude from the last column that $|\tan \kappa l_{ee}| \ll 1$ over most of $0 < b/\lambda_g < 0.5$. Thus we can eliminate the element l_{ee} as a good approximation, and write Lewin's equivalent circuit. Leaving out $\tan \kappa l_{ee}$, we obtain very simple expressions for the other elements of Fig. 2:

$$b \cong 1/H_{ss} = B_s \qquad \tan \kappa l_{oo} = 1/H_{oo} = B_o$$

$$n^2 \cong (H_{se}/H_{ss})^2 \cong H_{ee}/H_{ss} = B_s/B_e. \quad (18)$$

It is easy to ascertain that these approximate expressions agree with Lewin's expressions ((7a)–(7c)).

REFERENCES

[1] J T. Allanson, R Cooper and T. G. Cowling, "The theory and experimental behaviour of right-angled junctions in rectangular section waveguides," *JIEE*, vol. 93, pt. 3, No 23, pp. 177–187, May 1946.

[2] N. H. Frank and L J Chu, M. I. T Rad lab Report, Nos. 43-6 and 43-7, 1942.

[3] E D. Sharp, "An exact calculation for a T-junction of rectangular waveguides having arbitrary cross section," *IEEE Trans Microwave Theory Tech.*, vol MTT-15, pp. 109–116, Feb 1967.

[4] N. Marcuvitz, *Waveguide Handbook* New York: McGraw-Hill, 1951, ch 6.

[5] L Lewin, *Theory of Waveguides*. London Butterworth, 1975, pp. 291–301.

[6] C S Saxon, *Notes on Lectures by Julian Schwinger: Discontinuities in Waveguides*. New York: Gordon and Breach, 1968, pp 59, 101–102

Effect of a Cochannel Signal on the Electrical Tuning Characteristics of a Gunn Oscillator

B. N. BISWAS, S. SARKAR, AND S. CHATTERJEE,
STUDENT MEMBER, IEEE

Abstract—**New experimental observations on the pull-in as well as hold-in characteristics of an injection-locked microwave (Gunn) oscillator in the presence of a cochannel signal have been reported. The analytical treatment presented herein confirms the observations.**

I. INTRODUCTION

The effect of a cochannel signal on the performance of a microwave receiver has been studied in the past by a number of workers [1]–[5]. All these works indicate that the interfering signal reduces the tracking capability of an injection synchronized oscillator (ISO). However, experimental results in some cases show considerable departure from the existing concept. In [2] the effect of a low-strength interfering tone on the tracking behavior of an injection-locked oscillator has been considered, and naturally the amplitude perturbation of the oscillator has been neglected. This study found that the presence of interference induces asymmetry in the one-sided locking range of the oscillator. However, the two-sided locking range remains almost constant. In [3]–[5], however, the effect of large interference has been considered. It has been shown that the locking range decreases with an increase of the interference-to-carrier ratio. But it appears that detailed experimental observations on the performance characteristics of a microwave ISO, such as shift of the center frequency of the oscillator in the unlocked condition and the effect of amplitude perturbation on the locking behavior of an ISO in the presence of a cochannel signal having different detunings from the oscillator frequency, have not been reported. The purpose of the present paper is therefore to critically examine both theoretically and experimentally these characteristics, leading to some new findings.

II. EXPERIMENT

To study the effect of a cochannel signal on the performance characteristics of an ISO, an experimental arrangement as shown in Fig. 1(a) is set up. Here, a signal generator and a Gunn

Manuscript received October 31, 1987, revised September 12, 1988 This work was supported by the Department of Electronics of the Government of India

The authors are with the Radionics Laboratory, Department of Physics, Burdwan University, Burdwan 713 104, India

IEEE Log Number 8825386.